Supplementary information

Embedding atomic cobalt within hierarchical porous carbon derived from cross-linked polymers for high energy supercapacitors

Daba T. Bakhoum [a], Samba Sarr [a], Vusani M. Maphiri [a], Ndeye F. Sylla [a], Ndeye M. Ndiaye [b], Modou Diop [c], Balla D. Ngom [b], Mohamed Chaker [c] and Ncholu Manyala [a*]

[a] Department of Physics, University of Pretoria, Pretoria 0028, South Africa

[b] Laboratoire de Photonique Quantique, d'Energie et de Nano-Fabrication, Faculté des Sciences et Techniques Université Cheikh Anta Diop de Dakar (UCAD) B.P. 5005 Dakar-Fann Dakar, Sénégal

[c] Institut National de la Recherche Scientifique Centre-Énergie Matériaux Télécommunications 1650, Boulevard Lionel Boulet, Varennes, QC J3X 1S2, Canada*Corresponding author's email: ncholu.manyala@up.ac.za, Tel.: + (27)12 420 3549, Fax: + (27)12 420 2516

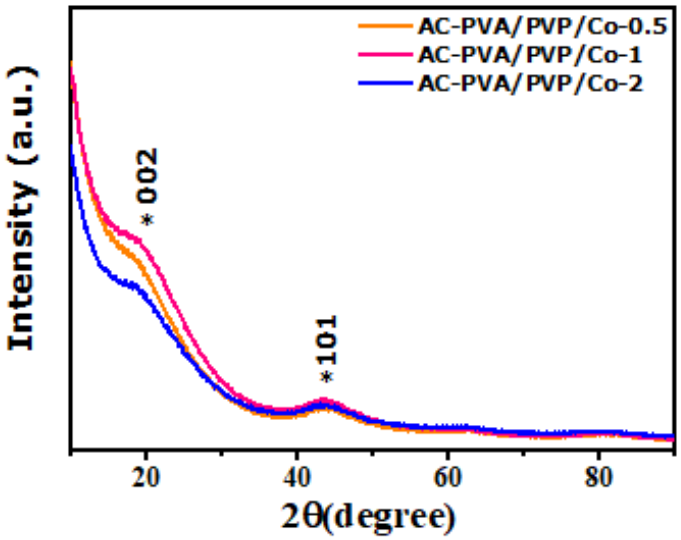

Fig. S1. XRD spectra of AC-PVA/PVP/Co-0.5, AC-PVA/PVP/Co-1, AC-PVA/PVP/Co-2 samples

The average crystallite size (L_a, nm) (or the average sp^2 cluster) via the Knight equation (S1) below:

$$L_a = \frac{C(\lambda)}{I_D/I_G} \quad \text{(S1)}$$

where C(λ) is the wavelength-dependent pre-factor estimated using $C(\lambda) \approx Co + \lambda C_1$, for $400 < \lambda < 700$ nm and $C(\lambda) = 4.96$ nm for $\lambda = 532$ nm, where C_0 and C_1 were estimated to be −12.6 nm and 0.033, respectively [1].

Table S1. BET data of activated carbon

Samples	**BET SSA (m^2g^{-1})**	**Total Pore Volume (cm^3g^{-1})**	**Micropore Volume (cm^3g^{-1})**	**Micropore SSA (m^2g^{-1})**
AC-PVA/PVP	1680	0.73	0.67	1604
AC-PVA/PVP/Co-0.5	1645	0.71	0.65	1587
AC-PVA/PVP/Co-1	1591	0.69	0.63	1520
AC-PVA/PVP/Co-2	1345	0.59	0.54	1289

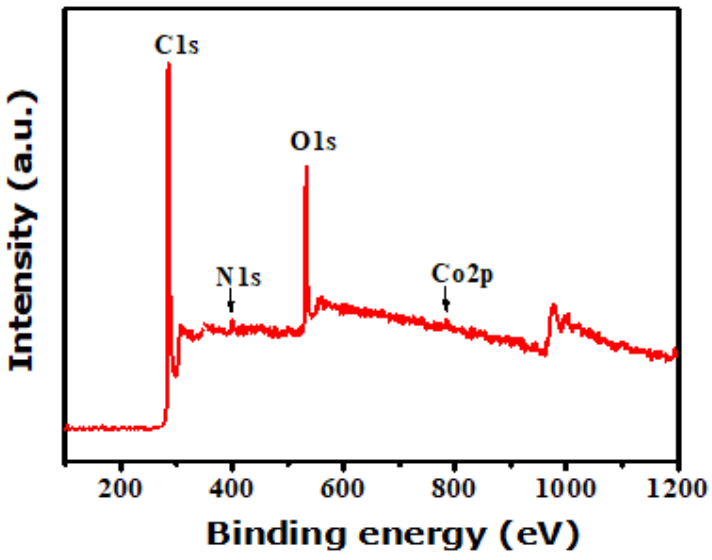

Fig. S2. XPS survey spectra of AC-PVA/PVP/Co-2

From the discharge process of the GCD, the specific capacitance C_{sp} (F. g^{-1}) of the as-prepared single half-cell electrode was calculated by using the formula stated in Eq. 2 [2]

$$C_{sp} = \frac{I\Delta t}{m\Delta V} \quad \ldots (S2)$$

Where I (mA) represents the charge/discharge current, ΔV (V) is the operating potential window, Δt (s) corresponds to the discharge time, m (mg) represents the mass of the active material electrodes.

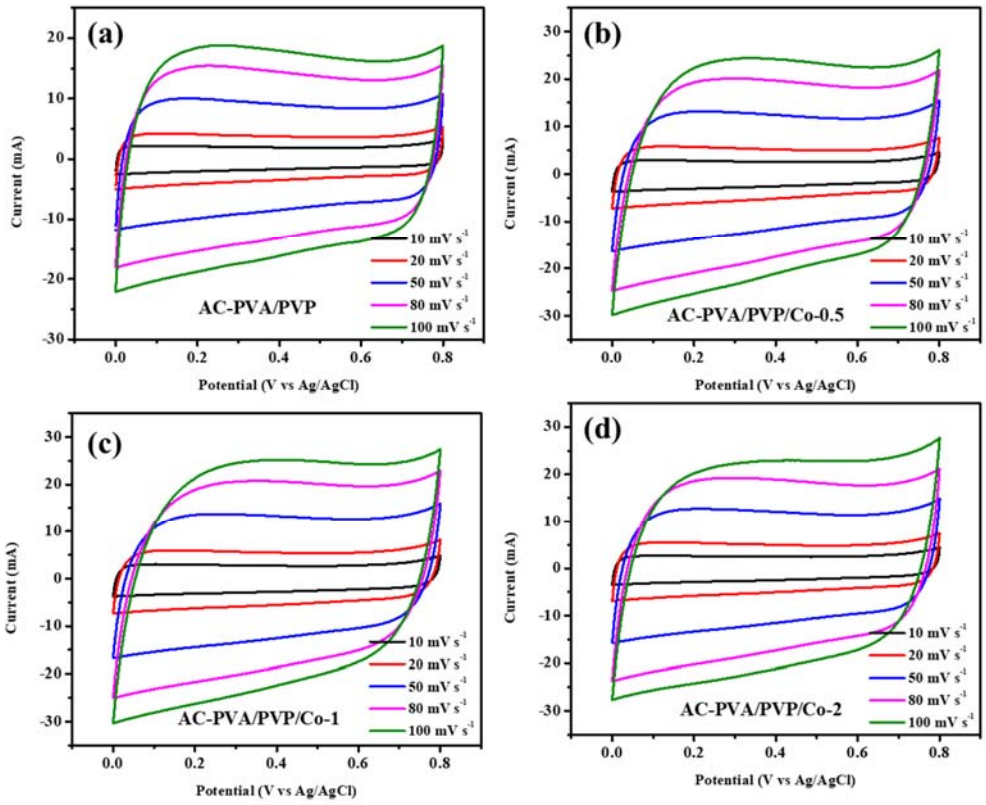

Fig. S3. CV curves at various scanning rate for the prepared samples

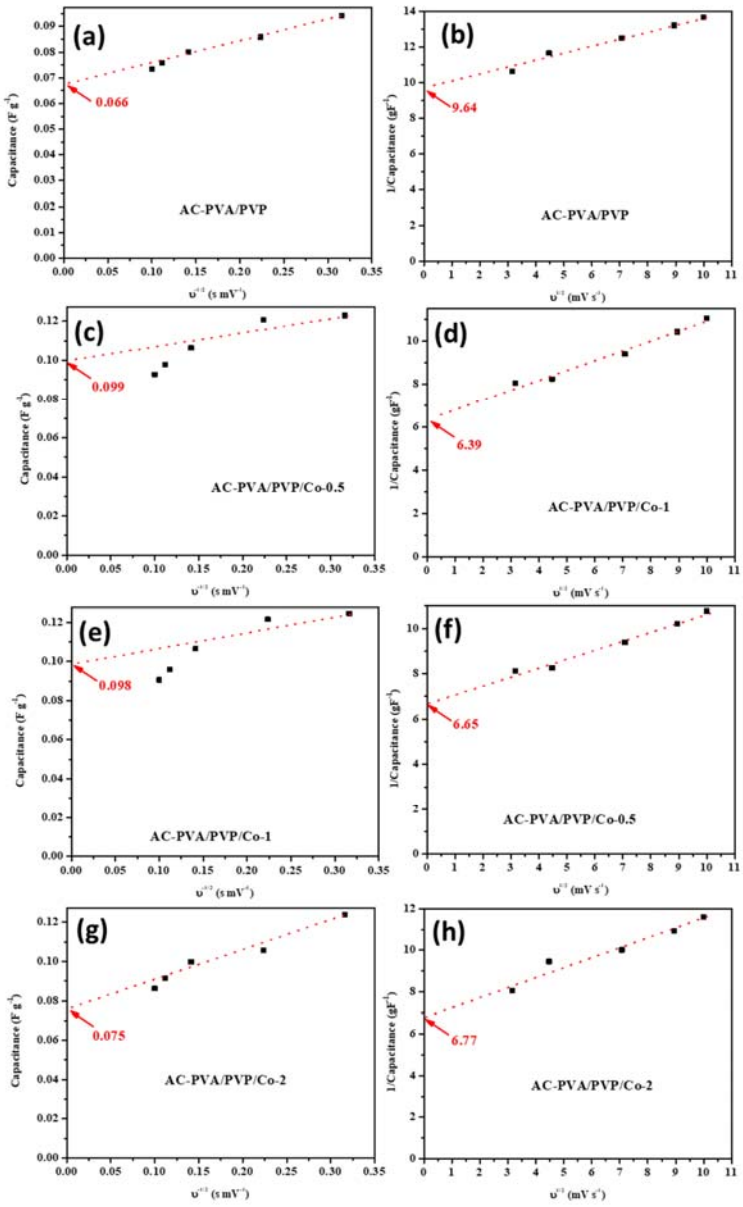

Figure S4. Trasatti's method for the prepared samples: (a,c,e,g) capacitance as a function of inverse square root of scan rate and (b,d,f,h) inverse capacitance as a function of square root of scan rate.

Equations (S3 – S5) was used to calculate the diffusion (C_{Pseudo}) contribution and the percentage of EDL and Pseudo capacitor.

$$C_T = C_{EDL} + C_{Pseudo} \quad \text{(S3)}$$

$$C_{EDL} = \frac{C_{EDL}}{C_T} \times 100 \quad \text{(S4)}$$

$$C_{Pseudo} = \frac{C_{Pseudo}}{C_T} \times 100 \quad \text{(S5)}$$

Table S2. Sample and values obtained from Transatti's method

Samples	CEDL	1\CT	CT	CPseudo	CEDL %	CPseudo %
AC-PVA/PVP	0.066	9.64	0.10373	0.037734	63.624	36.376
AC-PVA/PVP/Co-0.5	0.099	6.65	0.15037	0.051376	65.835	34.165
AC-PVA/PVP/Co-1	0.098	6.39	0.1563	0.058323	62.690	37.3094
AC-PVA/PVP/Co-2	0.075	6.77	0.1476	0.072623	50.805	49.195

C_T ~ total capacitance, C_{Pseudo} ~ pseudocapacitance and C_{EDL} ~ EDL capacitance

Table S3. Sample, ESR, R_{CT}.

Samples	ESR	R_{CT}
AC-PVA/PVP	1.80	0.30
AC-PVA/PVP/Co-0.5	1.14	0.48
AC-PVA/PVP/Co-1	1.10	0.50
AC-PVA/PVP/Co-2	1.35	0.45

From the discharge process of the GCD, the specific capacitance C_s (F. g^{-1}), specific energy (E, Wh kg^{-1}) and specific power (P, W g^{-1}) of the symmetric device were calculated according to Eqs. (S6), (S7) and (S8): [3]

$$C_s = \frac{I\Delta t}{m_T \Delta V} \quad \text{(S6)}$$

$$E_d = \frac{C_s(\Delta V)^2}{7.2} \quad \text{(S7)}$$

$$P_d = 3600\ \frac{E_d}{\Delta t} \quad \text{(S8)}$$

Where I (in A), Δt (in seconds), m_T (in g), ΔV (in V) represent respectively, the applied current, the discharging time from the GCD curves, the total mass of the electrode's material, the voltage windows.

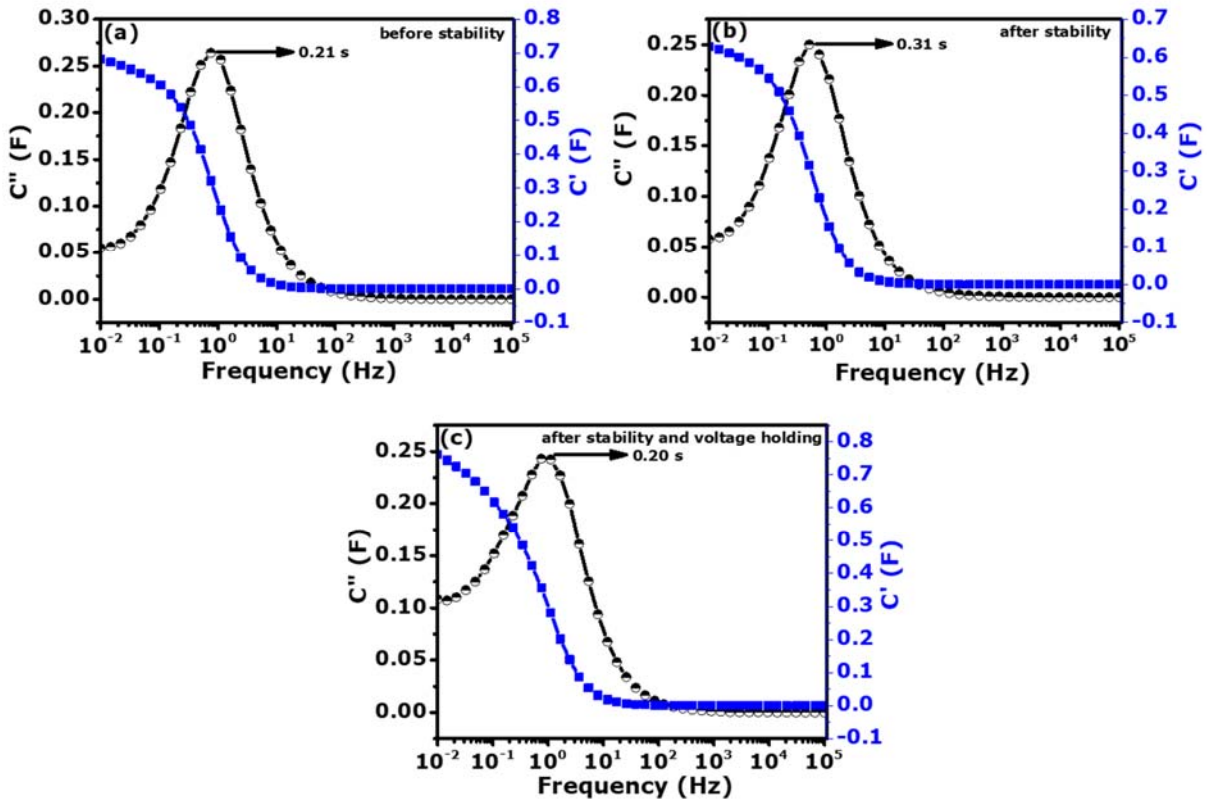

Fig. S5. Capacitance C' and C'' variation as function of the frequency (a) before stability, (b) after stability, (c) after stability and voltage holding

References

[1] V.M. Maphiri, D.T. Bakhoum, S. Sarr, N.F. Sylla, G. Rutavi, N. Manyala, Low temperature thermally reduced graphene oxide directly on Ni-Foam using atmospheric pressure-chemical vapour deposition for high performance supercapacitor application, J Energy Storage. 52 (2022) 104967. https://doi.org/10.1016/j.est.2022.104967.

[2] J.G. Kim, H.C. Kim, N.D. Kim, M.S. Khil, N-doped hierarchical porous hollow carbon nanofibers based on PAN/PVP@SAN structure for high performance supercapacitor, Compos B Eng. 186 (2020) 107825. https://doi.org/10.1016/j.compositesb.2020.107825.

[3] Y. Ding, J. Qi, R. Hou, B. Liu, S. Yao, J. Lang, J. Chen, B. Yang, Preparation of High-Performance Hierarchical Porous Activated Carbon via a Multistep Physical Activation Method for Supercapacitors, Energy and Fuels. 36 (2022) 5456–5464. https://doi.org/10.1021/acs.energyfuels.2c00688.